Molecular Simulation Study of the Effect of Pressure on the Vapor−Liquid Interface of the Square-Well Fluid

Jayant K. Singh and David A. Kofke*

Department of Chemical and Biological Engineering, University at Buffalo, The State University of New York, Buffalo, New York 14260-4200

Received November 15, 2004. In Final Form: February 28, 2005

We examine a model system to study the effect of pressure on the surface tension of a vapor−liquid interface. The system is a two-component mixture of spheres interacting with the square-well (A−A) and hard-sphere (B−B) potentials and with unlike (A−B) interactions ranging (for different cases) from hard sphere to strongly attractive square well. The bulk-phase and interfacial properties are measured by molecular dynamics simulation for coexisting vapor−liquid phases for various mixture compositions, pressures, and temperatures. The variation of the surface tension with pressure compares well to values given by surface-excess formulas derived from thermodynamic considerations. We find that surface tension increases with pressure only for the case of an inert solute (hard-sphere A−B interactions) and that the presence of A−B attractions strongly promotes a decrease of surface tension with pressure. An examination of density and composition profiles is made to explain these effects in terms of surface-adsorption arguments.

I. Introduction

The effect of pressure, p, on interfacial tension, γ, is an issue of longstanding interest.[1−7] The behavior is captured by the derivative

$$\tau \equiv \left(\frac{\partial \gamma}{\partial p}\right)_{\sigma,T,A} \tag{1}$$

where a change that occurs along the saturation curve (subscript σ) at constant temperature, T, and interfacial area, A, is indicated. From the phase rule, there is only one degree of freedom for two coexisting phases of a pure substance and thus one cannot vary saturation pressure at a fixed temperature; for a pure substance, τ is not defined. To proceed, it is necessary to consider a two-component system, for which the phase rule permits isothermal variation of the pressure while maintaining the presence of two phases. However, in this case, one still does not get a description of the purely mechanical effects that pressure has on surface tension. It is not possible to effect the change in pressure without also changing the species composition of the coexisting phases, which in turn can modify the composition and structure of the interfacial region. Thus, the effect of pressure on surface tension, when measured this way, is necessarily a result of the combined mechanical (pressure) and chemical (composition) effects. In the best case, an "inert" gas (insoluble in the liquid) is added to pressurize the system, which then produces changes in the vapor-phase composition only.

A Maxwell relation provides some insight that can be used to predict and understand the effect of pressure for a two-component system containing N_1 and N_2 molecules of species 1 and 2, respectively:

$$\left(\frac{\partial \gamma}{\partial p}\right)_{T,A,N_1,N_2} = \left(\frac{\partial V}{\partial A}\right)_{T,p,N_1,N_2} \tag{2}$$

The right-hand side describes the change in total volume that results from a change in the amount of interfacial area between the phases, keeping the overall mole numbers fixed. Rice[5] has discussed the effects giving rise to the change of volume. On one hand, movement of material from the bulk liquid to form the new surface (where the density is less) will result in an increase in the volume and tend to make the derivative positive. On the other hand, if vapor-phase molecules adsorb to some degree on the surface, then as new surface forms, it adsorbs more material from the vapor, causing the volume there to decrease and thus tend to make the derivative negative. In practice, both positive and negative values of τ have been observed in experiments involving the pressurization of a vapor−liquid interface using an inert gas, although negative values are much more prevalent.[7]

Hansen[8] presented a general formulation of interfacial thermodynamics, developed such that the pressure remains a relevant independent variable, while making both species chemical potentials into dependent variables. Turkevich and Mann[6] also showed how Hansen's construction could be used to determined τ strictly in terms of the volume and moles of the two-phase system and the densities of the bulk phases. Considering henceforth a mixture of two species only, a Gibbs−Duhem equation can be written for the composite liquid + vapor + interface system

$$-S\,\mathrm{d}T + V\,\mathrm{d}p - N_1\,\mathrm{d}\mu_1 - N_2\,\mathrm{d}\mu_2 - A\,\mathrm{d}\gamma = 0 \tag{3}$$

where S, V, and N_i are the total entropy, volume, and number of moles of species i in the two-phase system, respectively, and μ_i is the chemical potential of component i. To maintain equilibrium between the phases, an isothermal change in pressure must be accompanied by changes in the chemical potentials that permit them to

(1) Gibbs, J. W. *Collected Works* (Yale University Press: New Haven, 1906); Dover: New York, 1961; Vol. 1, p 236.
(2) Lewis, G. N.; Randall, M. *Thermodynamics and the Free Energy of chemical substances*; McGraw-Hill: New York, 1923; Chapter 21.
(3) Bridgman, P. W. *The Physics of High Pressure*; Beel: London, 1952.
(4) Defay, R.; Prigogine, I.; Bellemans, A.; Everett, D. H. *Surface Tension and Adsorption*; Wiley: New York, 1966; p 89.
(5) Rice, O. K. *J. Chem. Phys.* **1947**, *15*, 333.
(6) Turkevich, L. A.; Mann, J. A. *Langmuir* **1990**, *6*, 445.
(7) Turkevich, L. A.; Mann, J. A. *Langmuir* **1990**, *6*, 457.
(8) Hansen, R. S. *J. Phys. Chem.* **1962**, *66*, 410.

10.1021/la0471947 CCC: $30.25
Published on Web 03/30/2005

remain equal between the phases. These changes can be described by Gibbs−Duhem equations written separately for the two phases

$$-S^{\alpha}\,\mathrm{d}T + V^{\alpha}\,\mathrm{d}p - N_1^{\alpha}\,\mathrm{d}\mu_1 - N_2^{\alpha}\,\mathrm{d}\mu_2 = 0$$

$$-S^{\beta}\,\mathrm{d}T + V^{\beta}\,\mathrm{d}p - N_1^{\beta}\,\mathrm{d}\mu_1 - N_2^{\beta}\,\mathrm{d}\mu_2 = 0 \qquad (4)$$

with the phases indicated by the superscript (α or β). Alternatively,

$$V^{\alpha}(-s^{\alpha}\,\mathrm{d}T + \mathrm{d}p - n_1^{\alpha}\,\mathrm{d}\mu_1 - n_2^{\alpha}\,\mathrm{d}\mu_2) = 0$$

$$V^{\beta}(-s^{\beta}\,\mathrm{d}T + \mathrm{d}p - n_1^{\beta}\,\mathrm{d}\mu_1 - n_2^{\beta}\,\mathrm{d}\mu_2) = 0 \qquad (5)$$

where n_i is the molar density of species i in the bulk phase and s is the entropy density. By subtracting each of the equations given in eq 5 from eq 3 and dividing by the area, we obtain a Gibbs−Duhem equation that amplifies the effects of the interface

$$-\hat{s}\,\mathrm{d}T + \frac{1}{A}(V - V^{\alpha} - V^{\beta})\,\mathrm{d}p - \Gamma_1\,\mathrm{d}\mu_1 - \Gamma_2\,\mathrm{d}\mu_2 - \mathrm{d}\gamma = 0 \qquad (6)$$

where $\hat{s}$ is the surface-excess entropy. The surface excess of species i is defined as

$$\Gamma_i = (N_i - n_i^{\alpha}V^{\alpha} - n_i^{\beta}V^{\beta})/A \qquad (7)$$

At the level of detail where the interface is significant, the volumes V^{α} and V^{β} are ambiguous. Typically, they are defined to make two of the terms in eq 6 vanish. The most common definition is that due to Gibbs, for which $\Gamma_1 = 0$ and $V - V^{\alpha} - V^{\beta} = 0$. This definition has the advantage of conserving the total volume and permits the identification of a single plane that separates the two phases. In the present context, however, this definition is not helpful, as it obscures the influence of pressure on the other quantities. Instead, it is more useful to define the two molar excess properties to be zero: $\Gamma_1 = 0$ and $\Gamma_2 = 0$. With the volumes V^{α} and V^{β} defined this way, the derivative, τ, defined in eq 1 is precisely $(V - V^{\alpha} - V^{\beta})/A$. More specifically,[6]

$$\tau A = V - [(1 - \kappa_2)N_1/n_1^{\alpha} + (1 - \kappa_1)N_2/n_2^{\beta}]/(1 - \kappa_1\kappa_2) \qquad (8)$$

Here, the partition coefficients are defined as $\kappa_1 = n_1^{\beta}/n_1^{\alpha}$ and $\kappa_2 = n_2^{\alpha}/n_2^{\beta}$. This approach makes no reference to a dividing plane, but Turkevich and Mann have described how it can be connected to the Motomura two-plane approach.[9]

Equation 8 is subtle. It appears to describe a surface property in terms of purely bulk-phase properties, but this is not the case. Were we to ignore the interfacial effects and treat the phases as homogeneous with densities given everywhere by their bulk values, even very near the interface, we could write $N_1 = V(n_1^{\alpha}\phi + n_1^{\beta}(1 - \phi))$ and $N_2 = V(n_2^{\alpha}\phi + n_2^{\beta}(1 - \phi))$, where ϕ is the fraction of the total volume occupied by phase α. Substitution of these expressions in eq 8 yields, incorrectly, $\tau = 0$. When applied without this approximation, eq 8 yields a nonzero value of τ that includes elements that describe how the overall composition differs from a simple average of the bulk compositions.

While eq 8 has the benefit of being a rigorous expression for the pressure derivative of the surface tension, its connection to the equally rigorous eq 2 is not clear. The arguments given in connection to eq 2 relate to the excess solute at the surface, and this quantity is more naturally captured by the Gibbs definition of Γ_2 of eq 7. One can proceed less easily but still rigorously from this standpoint too. Using the Gibbs convention for V^{α} and V^{β}, we write

$$\tau = -\Gamma_2\left(\frac{\partial\mu_2}{\partial p}\right)_{\sigma,T} \qquad (9)$$

The derivative here can be given in terms of the bulk-phase properties using an analysis similar to that leading to the Clapeyron equation.[10] The result is

$$\left(\frac{\partial\mu_2}{\partial p}\right)_{T,\sigma} = \frac{n_1^{\beta} - n_1^{\alpha}}{n_1^{\beta}n_2^{\alpha} - n_1^{\alpha}n_2^{\beta}} \approx \frac{1}{n_2^{\beta}} \qquad (10)$$

where the approximate equality is based on the assumptions that the amount of solute in the liquid is negligible ($n_2^{\alpha} \approx 0$) and that the liquid-phase density of solvent is greater than its vapor-phase density ($n_1^{\alpha} \gg n_1^{\beta}$); the indication is that the derivative is positive. Combination of eqs 9 and 10 indicates that the slope, τ, is of opposite sign to the surface excess of species 2. Thus, adsorption of solute on the surface (indicated by positive Γ_2) from the vapor promotes the decrease of surface tension with pressure, as argued in the context of eq 2.

Molecular simulations have been applied to understand surface behavior in a variety of contexts.[11,12] Such studies can be useful in probing molecular-level aspects of surface phenomena. Modeling studies are also of interest for their ability to examine systematically how qualitative features of molecular interactions influence surface properties. As it involves the effect of solutes on surface behavior, adsorption of a volatile component can significantly reduce the surface tension, as shown by Lee et al.[13] Interesting behavior was also noticed by Lee et al. for a low ratio of solute/solvent diameter. As the adsorption is very little at the interface, under such conditions, surface tension increases with an increase in the composition of solute. Several others[14−17] also studied the vapor−liquid interface of binary mixtures. However, the issue of the effect of pressure on surface tension has not been explored previously with these techniques.

In this work, we study the effect of pressure on surface tension for some model binary systems. In particular, we examine the vapor−liquid interfacial properties for the

(9) Motomura, K.; Aratano, M. *Langmuir* **1987**, *3*, 304.

(10) Denbigh, K. *Principles of Chemical Equilibrium*, 4th ed.; Cambridge University Press: Cambridge, U.K., 1971.

(11) Rowlinson, J. S.; Widom, B. *Molecular Theory of Capillarity*; Oxford University Press: Oxford, U.K., 1982.

(12) Croxton, C. A. *Statistical Mechanics of the Liquid Surface*; Wiley: New York, 1980.

(13) Lee, D. J.; daGamma, M. M. T.; Gubbins, K. E. *J. Phys. Chem.* **1985**, *89*, 1514.

(14) Lee, D. J.; daGamma, M. M. T.; Gubbins, K. E. *Mol. Phys.* **1984**, *53*, 1113.

(15) Salomons, E.; Mareschal, M. *J. Phys.: Condens. Matter* **1991**, *3*, 3645.

(16) Salomons, E.; Mareschal, M. *J. Phys.: Condens. Matter* **1991**, *3*, 9215.

(17) Mecke, M.; Winkelmann, J.; Fischer, J. *J. Chem. Phys.* **1999**, *110*, 1188.

square-well (SW) model, in the presence of solutes of varying degree of attraction for the SW solvent. We demonstrate the effects discussed above, namely, that the surface tension increases with pressure for a truly inert solute but that even a modest degree of attraction can cause τ to become negative. We also use the detailed information provided by simulation to test eq 8 for τ, which is not as easily implemented using experimental data. The rest of this paper is organized as follows. In the next section, we give details about the models and simulations performed in this study. Then, in section 3, we present and discuss the results. We conclude in section 4.

II. Model and Methods

The model chosen in this study is a liquid−vapor system of square-well (SW) particles. The SW potential is arguably the simplest model that incorporates both repulsive and attractive forces between molecules. It is defined by the pair energy, $u(r)$:

$$u(r) = \begin{cases} \infty, & 0 < r < \sigma \\ -\epsilon, & \sigma \le r < \lambda\sigma \\ 0, & \lambda\sigma \le r \end{cases} \tag{11}$$

where $\lambda\sigma$ is the potential-well diameter, ϵ is the depth of the well, and σ is the diameter of the hard core. Because of its simplicity and analytic tractability, the SW potential has been applied as a model of simple atomic systems,[18−20] colloidal particles,[21−24] heterochain molecules,[25,26] and complex systems,[27−29] among others.

In the present study, all systems employed $N = 1000$ particles of which the x_{sw} fraction of the molecules were square-well solvent species (A) and the rest were solute particles (B). All hard-core diameters were set equal, that is, $\sigma_{AA} = \sigma_{AB} = \sigma_{BB} \equiv \sigma$. The solute particles interacted only as hard spheres ($\epsilon_{BB} = 0$, no attraction), and the solvent SW parameters were the same for all systems studied here. A range of values for the solute−solvent interaction was examined, from purely repulsive with no attraction ($\epsilon_{AB} = 0$) to highly attractive ($\epsilon_{AB} = 2.0$). In this and all that follows, properties are given in units such that σ and ϵ_{AA} are unity.

A common method to calculate surface tension by molecular simulation is by placing a slab of fluid in a rectangular simulation cell with periodic boundaries, such that the fluid spans the short (x, y) dimensions of the simulation volume.[30] The z-axis is extended to produce the vapor phase, and the system is allowed to equilibrate to create a vapor space before taking the averages of the properties of interest. We adopted this approach for the present study. The thermodynamic definition of the surface tension, γ, expresses it in terms of the change in free energy, F, as the interfacial area, A, of two coexisting phases is changed at constant volume, V,

$$\gamma = \left(\frac{\partial F}{\partial A}\right)_{T,V,N} \tag{12}$$

From this definition, we can show that the surface tension can be expressed in terms of components of the pressure tensor for the slab based geometry

$$\gamma = \frac{L_z}{2}\left\langle p_{zz} - \frac{1}{2}(p_{xx} + p_{yy})\right\rangle \tag{13}$$

where $p_{\alpha\alpha}$ is the $\alpha\alpha$ component of the pressure tensor. The factor of $^1/_2$ multiplying the average accounts for the presence of two interfaces in the system. L_z is the extended length of the box.

Pressure-tensor components can be obtained from the virial.[30] For pairwise-additive potentials, the expression is

$$p_{\alpha\beta} = \rho kT + \frac{1}{V}\left\langle \sum_{i=1}^{N-1}\sum_{j>i}^{N} (\mathbf{r}_{ij})_\alpha (\mathbf{f}_{ij})_\beta \right\rangle \tag{14}$$

where N is the total number of molecules, ρ is the number density, k is the Boltzmann constant, T is the temperature, $\mathbf{r}_{ij}$ is the vector between the center of mass of molecules i and j, and $\mathbf{f}_{ij} = -\nabla u_{ij}$ is the force between them; the angle brackets indicate an ensemble or time average. For hard potentials such as those used in this study, the forces are impulsive, having infinite magnitude but acting for an infinitesimal time. When integrated over time, each collision contributes a well-defined amount to the average in eq 14

$$p_{\alpha\beta} = \rho kT + \frac{1}{V t_{sim}} \sum_{\text{collisions}} (\mathbf{r}_{ij})_\alpha (\Delta\mathbf{p}_{ij})_\beta \tag{15}$$

where t_{sim} is the total simulation time and the sum is over all collisions occurring in this time; $\Delta\mathbf{p}_{ij}$ is the impulse associated with the collision between atoms i and j. The simulation proceeds in the usual manner for impulsive potentials:[30] solve for the time when the next pair collides (which occurs when any two particles reach a separation equal to the hard-core or square-well diameters), advance each particle to that time via free-flight kinematics, process the dynamics of the colliding pair, and move on to the next collision to repeat the process. With each collision, a contribution to the pressure-tensor averages is made in accordance with eq 15.

Our molecular dynamics (MD) simulations were performed in a canonical (NVT) ensemble, that is, at a prescribed total particle number (liquid + vapor + interface), total volume, and temperature. The simulation was started from a face-centered-cubic lattice configuration in a cubic periodic box. The initial overall density was fixed at $\rho\sigma^3 = 0.84$, from which we created a vacuum by expanding the box in one dimension, such that the final dimension of the box had $L_x = L_y = 10\sigma$ and $L_z = 4 \times L_x$. The temperature was kept constant by simple momentum scaling. The simulations were equilibrated for 1.3 million time steps, and averages were taken for around 400 000 time steps (where the time step is $\Delta t = 0.02\sigma_{AA}\sqrt{m/\epsilon_{AA}}$, with m being the particle mass; this step is given only as a convenient measure of the length of the simulation, and it has no effect on the dynamics. Typically, multiple collisions will occur in a single Δt).

(18) Del Rio, F.; Delonngi, D. A. *Mol. Phys.* **1985**, *56*, 691.
(19) Vega, L.; de Miguel, E.; Rull, L. F.; Jackson, G.; McLure, I. A. *J. Chem. Phys.* **1992**, *96*, 2296.
(20) Chang, J.; Sandlar, S. I. *Mol. Phys.* **1994**, *81*, 745.
(21) Bolhuis, P.; Frenkel, D. *Phys. Rev. Lett.* **1994**, *72*, 2211.
(22) Asherie, N.; Lomakin, A.; Benedek, G. B. *Phys. Rev. Lett.* **1996**, *77*, 4832.
(23) Noro, M. G.; Frenkel, D. *J. Chem. Phys.* **2000**, *113*, 2941.
(24) Zaccarelli, E.; Foffi, G.; Dawson, K. A.; Sciortino, F.; Tartaglia, P. *Phys. Rev. E* **2001**, *63*, 031501.
(25) Cui, J.; Elliot, J. R. *J. Chem. Phys.* **2001**, *114*, 7283.
(26) McCabe, C.; Gil-Villegas, A.; Jackson, G.; Del Rio, F. *Mol. Phys.* **1999**, *97*, 551.
(27) Lomakin, A.; Asherie, N.; Benedek, G. B. *J. Chem. Phys.* **1996**, *104*, 1646.
(28) Zhou, Y.; Karplus, M.; Ball, K. D.; Berry, R. S. *J. Chem. Phys.* **2002**, *116*, 2323.
(29) Zhou, Y.; Karplus, M.; Wichert, J. M.; Hall, C. K. *J. Chem. Phys.* **1997**, *107*, 10691.
(30) Allen, M. P.; Tildesley, D. J. *Computer Simulation of Liquids*; Oxford University Press: Oxford, U.K., 1987.

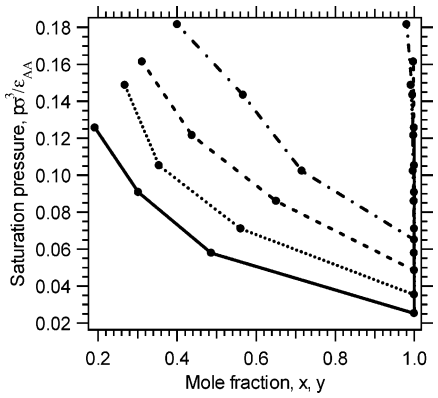

Figure 1. Vapor–liquid coexistence diagram for the $\epsilon_{AB} = 0$ (hard-sphere) mixture, showing coexisting liquid, x, and vapor, y, solvent mole fractions for various pressures. The lines describe data for different temperatures: 1.0 (bottom), 1.05, 1.1, and 1.15 (top).

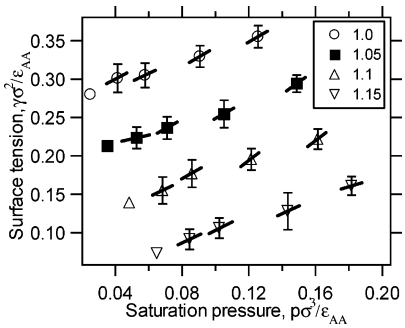

Figure 2. Surface tension versus saturation pressure for the $\epsilon_{AB} = 0$ mixture. Temperatures, kT/ϵ_{AA}, are indicated in the legend. The short slanted lines through each point have a slope equal to τ, as given in eq 8.

The phase coexistence point was adjusted by varying the overall composition of the system. A fixed number of solvent atoms (ranging from 700 to 1000) and solute atoms (from 300 to 0) were introduced, and the vapor and liquid densities and compositions were permitted to adopt their equilibrium values. The resulting pressure was measured by averaging the virial.

III. Results and Discussion

We consider first a system in which the solute has no attraction to the solvent, so that solute–solute and solute–solvent interactions are pure hard sphere. This system is a true example of the inert gas that is sometimes approximated experimentally when focusing on the effect of pressure on surface tension. We examined the behavior for four temperatures—T (in units of ϵ_{AA}/k) = 1.0, 1.05, 1.1, and 1.15—and with solvent–solvent square-well parameters $\lambda = 1.5$ and 2.0 (in separate studies); we present detailed results for the $\lambda = 1.5$ case only, as the results for $\lambda = 2.0$ are qualitatively similar. Figure 1 presents a portion of a pressure–composition (p–xy) coexistence diagram as determined using the vapor + liquid simulations described above. The amount of hard-sphere solute in the liquid phase is negligibly small.

The surface tension for the hard-sphere solute system is presented as a function of pressure and temperature in Figure 2, along with data for the pure square-well system taken from previous work.[31] The temperature dependence is as expected, with the surface tension decreasing smoothly with increasing temperature. As for the pressure dependence, this system exhibits the uncommon behavior in which surface tension increases with pressure. This outcome could be anticipated on the basis of the arguments reviewed above, relating the pressure dependence to the volume change accompanying the creation of interfacial area (eq 2). For this system, an increase in area results in an increase in volume (at fixed pressure), because the new area takes liquid and moves it to the lower-density interface. There is no competing effect of adsorption of solute at the interface, because the solute is completely inert. It would seem that this behavior is described well through examination of the density and composition profiles, which are presented in Figure 3 for $T = 1.0$. It is evident from the figure that there is indeed a marked *depletion* of solute at the interface. The solvent mole fraction in the vapor is significantly enhanced in the vicinity of the interface (as defined by the density variation). However, we will revisit this issue below and find that the picture presented by Figure 3 gives an inadequate representation of the relevant effects.

Table 1. Surface Tension, γ, Its Pressure Derivative, τ, According to eq 8, and the Gibbs Surface Excess, Γ_2[a]

		$\epsilon_{AB} = 0.0$			$\epsilon_{AB} = 0.5$		
x_A	T	γ	τ	Γ_2	γ	τ	Γ_2
0.7	1.0	0.36(1)	1.24	−0.10	0.19(1)	−1.81	0.13
0.7	1.05	0.29(1)	1.64	−0.14	0.12(1)	−1.21	0.087
0.7	1.1	0.22(1)	1.65	−0.14	0.011(7)	−0.73	0.033
0.7	1.15	0.16(1)	0.67	−0.059			
0.8	1.0	0.33(1)	1.24	−0.073	0.21(2)	−1.83	0.092
0.8	1.05	0.25(2)	1.23	−0.073	0.16(1)	−2.69	0.13
0.8	1.1	0.20(1)	1.61	−0.098	0.089(9)	−1.75	0.086
0.8	1.15	0.13(2)	0.90	−0.055			
0.9	1.0	0.30(2)	1.11	−0.034	0.25(1)	−2.90	0.073
0.9	1.05	0.24(1)	1.38	−0.044	0.18(1)	−1.75	0.046
0.9	1.1	0.18(2)	1.02	−0.032	0.12(1)	−2.06	0.051
0.9	1.15	0.11(1)	0.94	−0.031			
0.95	1.0	0.30(2)	1.27	−0.020	0.27(1)	−3.07	0.040
0.95	1.05	0.22(1)	0.48	−0.0075	0.20(1)	−2.44	0.033
0.95	1.1	0.16(2)	0.98	−0.016	0.15(1)	−1.97	0.026
0.95	1.15	0.091(13)	0.92	−0.015			

[a] The data are given for different temperatures, T (in units of ϵ_{AA}/k), and overall (liquid + vapor + interface) solvent mole fraction, x_A. All other quantities are given in units such that σ_{AA} and ϵ_{AA} are unity. The numbers in parentheses indicate the 67% confidence limits of the last digit(s) of the tabled value.

Figure 2 gives an indication of the slope $\tau = (\partial\gamma/\partial p)_T$ according to the Hansen–Turkevich–Mann formula given above as eq 8. The small lines on each data point indicate the slope expected from the formula, and they show an imperfect but still satisfactory agreement with the overall behavior of the γ versus p curves. The values of τ computed this way are presented in Table 1. This quantity derives its value from an imbalance between the number of molecules in the system versus the number given in terms of the bulk densities, and consequently, its evaluation requires precise knowledge of the bulk-phase densities and the numbers of molecules of each species in the phase. Of course in a simulation, the molecule numbers are known exactly and the densities are given rather precisely also. One might consider in this context how well this calculation could be completed using experimentally obtained data. To aid in this evaluation, we have performed a sensitivity analysis, in which we computed $\partial \ln \tau/\partial \ln x$, where x is any of the quantities appearing in eq 8. This derivative describes, roughly, what percent change in τ can be expected from a 1% change (or error) in each quantity. We find that this derivative is of the order of 20 or so (i.e., τ changes by 20% for a 1% change in the quantity)

(31) Singh, J. K.; Kofke, D. A.; Errington, J. R. *J. Chem. Phys.* **2003**, *119*, 3405.

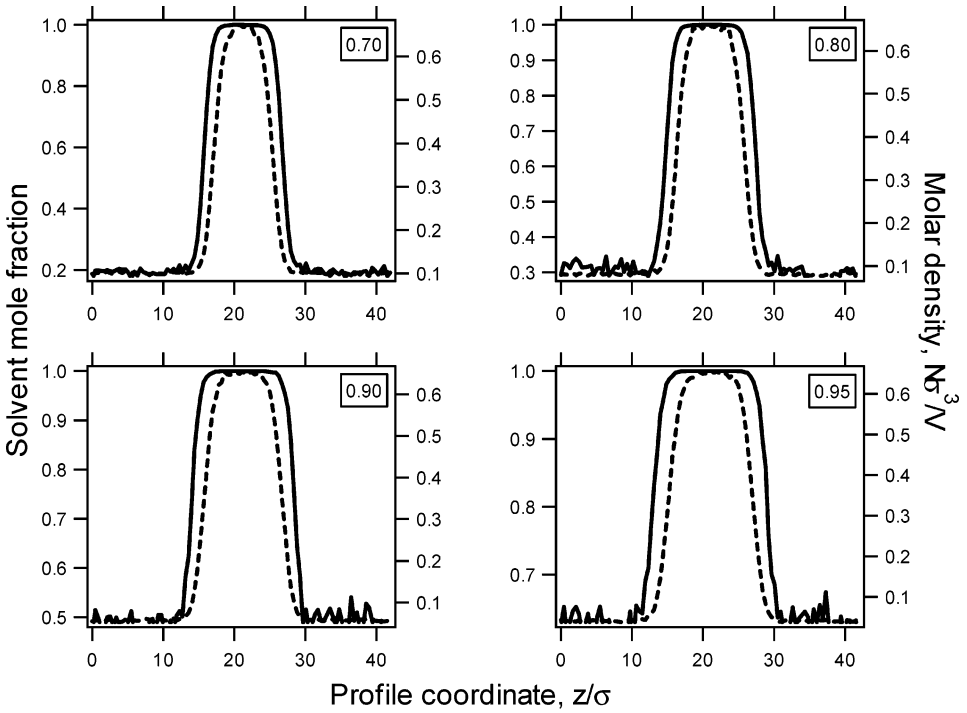

Figure 3. Profiles of solvent mole fraction (solid line) and total molar density (dashed line) for various compositions of the $\epsilon_{AB} = 0$ mixture at $T = 1.0$. The overall mole fraction (vapor + liquid + interface) for square-well (A) species is given in the inside box.

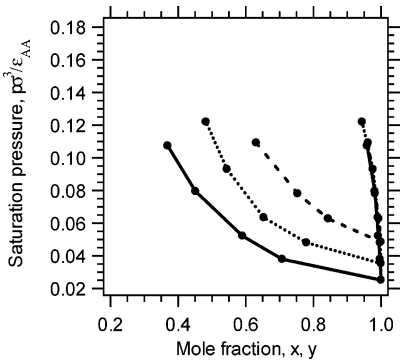

Figure 4. Vapor−liquid coexistence diagram for the $\epsilon_{AB} = 0.5$ mixture. The lines describe data for different temperatures: 1.0 (bottom), 1.05, and 1.1 (top).

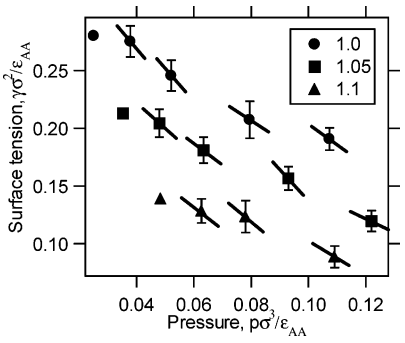

Figure 5. Surface tension versus saturation pressure for the $\epsilon_{AB} = 0.5$ mixture. Temperatures, kT/ϵ_{AA}, are indicated in the legend. The short slanted lines through each point have a slope equal to τ, as given in eq 8.

for almost all of the independent variables, indicating that the τ value calculated this way is indeed sensitive to the quality of these data. The noise in the slopes depicted in Figure 2 is consistent with this observation.

To examine the effect of solvent (A)−solute (B) interaction on the surface tension, we repeated the calculations described above for the SW−HS mixture but with an A−B interaction that is mildly attractive ($\epsilon_{AB} = 0.5$). The B−B interaction remains purely repulsive. Figure 4 presents a portion of the phase diagram for the $\epsilon_{AB} = 0.5$ system. Perhaps its most notable feature is that it is not qualitatively different from the SW−HS behavior shown in Figure 1. The mole fraction of solute in the liquid is slightly more, but overall, the form of the coexistence envelopes is very similar to that seen in Figure 1.

In light of the great similarities in the phase diagrams for this and the SW−HS systems, it is interesting to observe qualitatively different behaviors in the surface tension versus pressure. Figure 5 presents these data. The slope has changed sign, and the system now exhibits the more common behavior of decreasing surface tension with pressure. The small attraction added to the solute−solvent interactions is quite sufficient to change the phenomenology. This outcome explains well why most real systems (i.e., any not involving a helium solute) exhibit a negative τ value; it simply does not take much solute−solvent attraction to cause the surface tension to decrease with pressure. Slopes according to eq 8 are again indicated on the figure and agree acceptably with the shape of the curves. The sensitivities of the slopes to the parameters of the equation are listed in Table 2. Roughly the same degree of sensitivity is seen as in the previous example.

Given the qualitative change in the pressure dependence of γ, one might expect to see a stark change in the concentration and density profiles. However, we do not, as shown in Figure 6. There remains a significant layer of solvent enhancement in the vapor near the interface, which itself is not surprising given the stronger affinity of the solvent molecules for the (solvent-dominated) liquid phase. A more illuminating picture examines the behavior of the solvent and solute profiles together. These behaviors can connect to the surface excess, Γ_2, which was shown by eqs 9 and 10 to relate simply to τ for the type of system presently under study. Figures 7 and 8 are the relevant

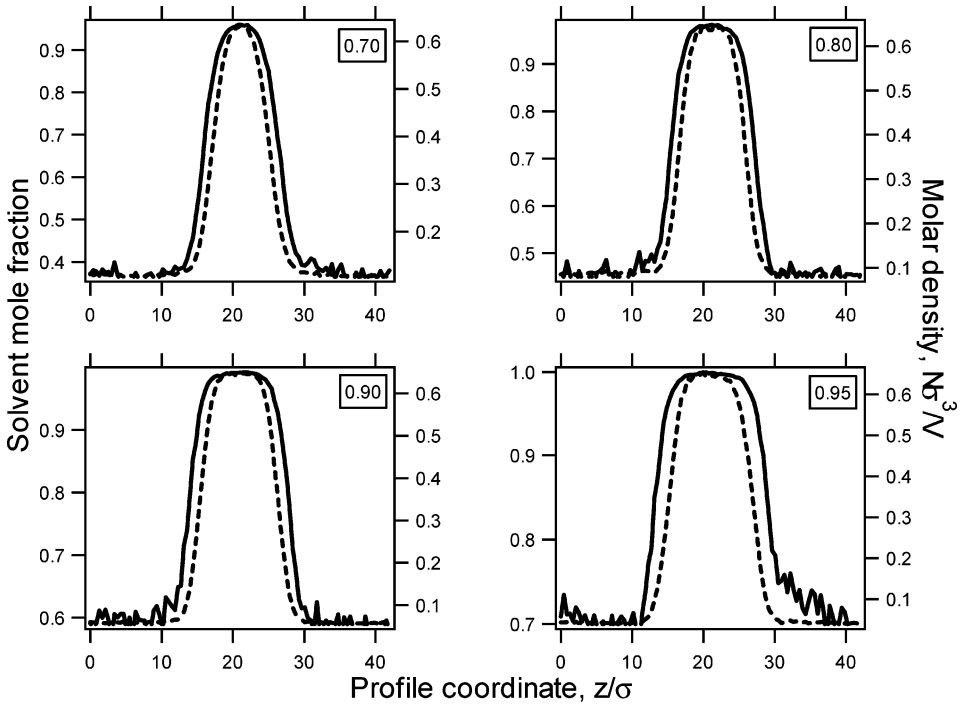

Figure 6. Profiles of solvent mole fraction (solid line) and total molar density (dashed line) for various compositions of the $\epsilon_{AB} = 0.5$ mixture at $T = 1.0$. The overall mole fraction (vapor + liquid + interface) for the square-well (A) species is given in the inside box.

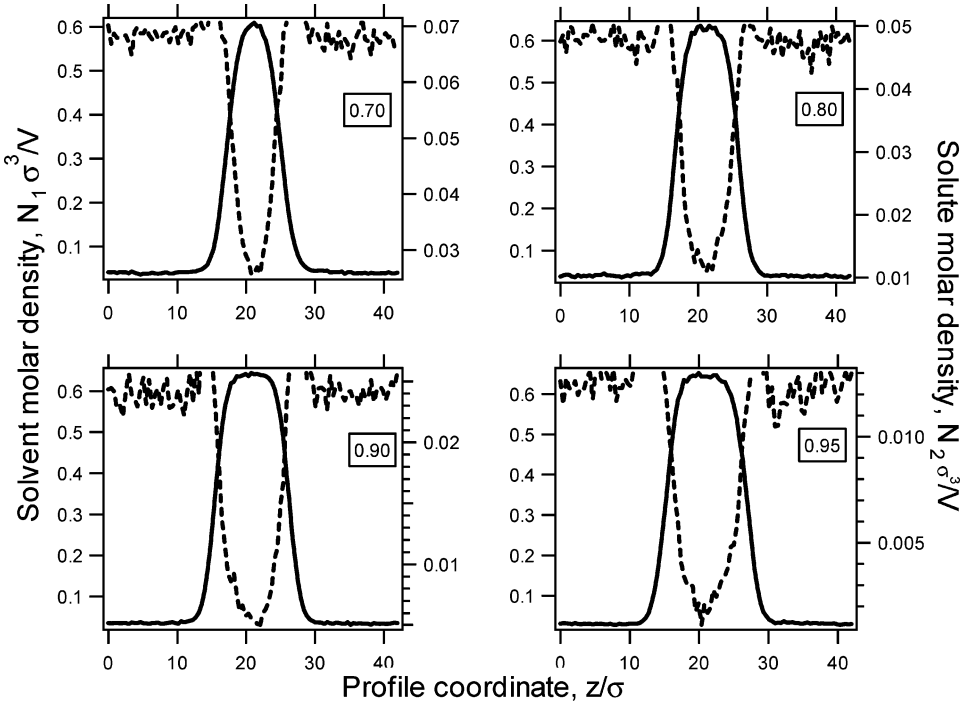

Figure 7. Profiles of solvent molar density (solid line) and solute molar density (dashed line) for various compositions of the $\epsilon_{AB} = 0.0$ mixture at $T = 1.0$. The overall composition (vapor + liquid + interface) for the square-well (A) species is given in the inside box.

plots. These figures show the species density profiles, $n_1(z)$ and $n_2(z)$. At first glance, they too do not seem to differ, but there is a feature that is consistently different between them. The figures are scaled such that each profile covers its full range, and no more, for the range of the ordinate axes. When presented this way, the point at which the two profiles cross can give some indication of their relative rate of change. In Figure 7, presenting results for the square-well solute, one finds that the curves cross toward the upper half of the scale. This indicates the solute profile is changing more rapidly than the solvent profile. A more rapid rise in solute concentration corresponds to an enhancement of solute at the interface. In contrast, the profiles for the hard-sphere solute, shown in Figure 8, show that the curves cross toward the lower half of the scale. This means that the solute concentration is rising slowly compared to the drop in solvent concentration, and the interface is relatively depleted of solute. These

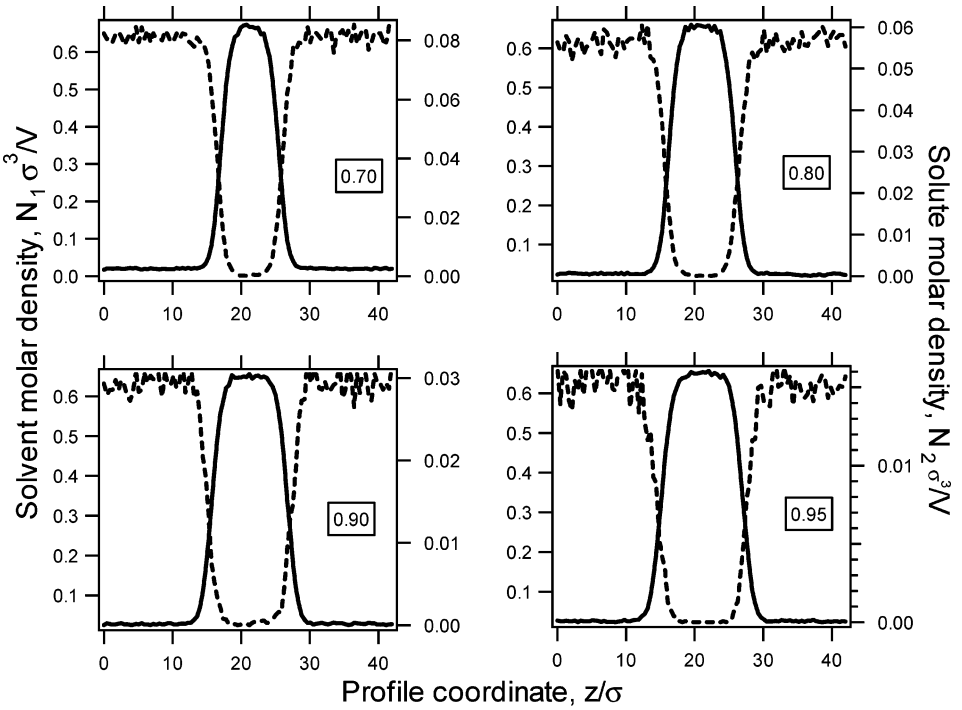

Figure 8. Profiles of solvent molar density (solid line) and solute molar density (dashed line) for various compositions of the $\epsilon_{AB} = 0.5$ mixture at $T = 1.0$. The overall composition (vapor + liquid + interface) for the square-well (A) species is given in the inside box.

Table 2. Surface Tension, γ, Its Pressure Derivative, τ, and Sensitivity Measures of τ with Respect to n_a (solvent number density in liquid), n_b (solute number density in vapor), N_a (total number of solvent particles), and N_b (total number of solute particles)[a]

ϵ_{AB}	γ	τ	$\partial \ln \tau / \partial \ln n_a$	$\partial \ln \tau / \partial \ln n_b$	$\partial \ln \tau / \partial \ln N_a$	$\partial \ln \tau / \partial \ln N_b$
0	0.36(1)	1.2	6.7	26	−7.5	−26
0.5	0.19(1)	−1.8	−2.7	−19	3.6	21
1	0.21(1)	−5.9	9.2	−8.3	−11	19
1.2	0.30(2)	−10	22	−6.5	−24	29
1.4	0.43(2)	5.9	−290	15	300	−310
1.6	0.61(3)	37	130	0.7	−130	130
1.8	0.89(4)	−37	−66	0.7	69	−67
2	1.03(3)	−11	−190	0.4	200	−190

[a] The data are for systems with different solvent−solute well-depth parameters, ϵ_{AB}, at a temperature of $kT/\epsilon_{AA} = 1.0$ and an overall solvent mole fraction of $x_A = 0.7$. All values are given in units such that σ_{AA} and ϵ_{AA} are unity. The numbers in parentheses indicate the 67% confidence limits of the last digit of the tabled value.

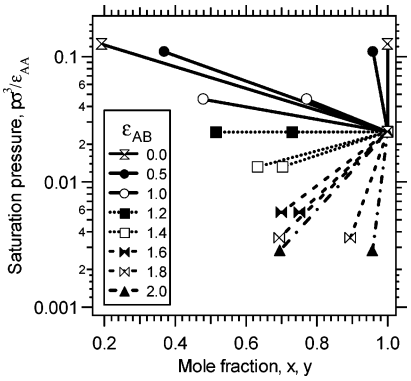

Figure 9. Vapor−liquid coexistence diagram for several mixtures differing in ϵ_{AB}, as indicated. The lines join a single pair of coexistence points (each for a system of an overall mole fraction (vapor + liquid + interface) of 0.7) to a common coexistence point for the pure-solvent system. All data are for $T = 1.0$.

considerations are quantified by the Gibbs surface excess, Γ_2, which does indeed exhibit different signs for the two cases. Data are given in Table 1.

One might consider quantifying the behavior captured in Figures 7 and 8 by fitting the profiles to a suitable functional form. Differences in the rates of change of the profiles for each component would yield different interface thicknesses in such fits, and these differences might be connected to the behavior of τ. The square-gradient model of Cahn and Hilliard[32] leads to a hyperbolic-tangent form for the density profile

$$y(z) = \bar{y} + \Delta y \tanh(z/\xi) \qquad (16)$$

where y is a property that varies across the interface, $\bar{y} = (y^\alpha + y^\beta)/2$ and $\Delta y = (y^\alpha - y^\beta)/2$. The parameter ξ is a correlation length that describes the rate of change of y across the interface. One of the assumptions used in developing eq 16 is that only a single intensive property varies across the interface. Thus, it may be appropriate to use only for single-component vapor−liquid interfaces (for which y stands for the density) or two-component liquid−liquid interfaces (for which y stands for the mole fraction), and such systems. In the present case, both the density and the composition change across the interface. Thus, while eq 16 has the appropriate qualitative form to describe the profiles in Figure 7, in important ways, it might be expected to be inadequate. Indeed, if eq 16 is used to describe $n_1(z)$ and $n_2(z)$ (each with its own ξ), eq 8 yields $\tau \equiv 0$. Alternatively, if instead eq 16 is used to describe both the overall density, $\rho(z)$, and the mole fraction, $c(z)$ (again each with its own value of ξ), then eq 8 shows that τ is necessarily negative. These restrictions are not obeyed in all of our results, so a simple application of eq 16 cannot give a correct quantitative description of the profiles (at least for $\tau > 0$), so it cannot be used to interpret Figures 7 and 8.

(32) Cahn, J. W.; Hilliard, J. E. *J. Chem. Phys.* **1958**, *28*, 258.

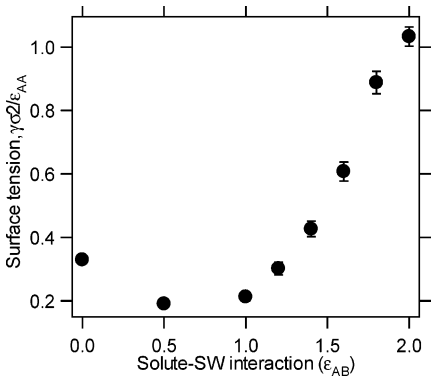

Figure 10. Surface tension of a square-well fluid in the presence of solute with varying solute−solvent interaction at a constant temperature, $T = 1.0$. The overall mole fraction (vapor + liquid) of square-well molecule is fixed at 0.7.

We finish this work with a broader, less-detailed examination of the effect of the solute−solvent interaction, ϵ_{AB}, on the surface tension and its pressure derivative. For this part of the study, we look at a single temperature of $T = 1.0$ and an overall solvent mole fraction of 0.7. Within these constraints, we varied ϵ_{AB} from 1.0 to 2.0 in steps of 0.2, supplementing the corresponding data already considered for $\epsilon_{AB} = 0$ and 0.5. An outline of the $p-xy$ behavior available from these data is shown in Figure 9. This figure presents on a single plot a coarse-grained picture of the dilute vapor−liquid coexistence behavior of all of the systems. Two coexistence states are given for each system (one being the pure solvent at $x, y = 1$), and the lines give a rough, imperfect picture of the coexistence region between these points. The increased solute−solvent attraction results in a clear enrichment of the liquid phase. For $\epsilon_{AB} > 1.2$, the liquid composition is practically equal to the overall composition, and in these cases, each system is at its bubble point. These systems all exhibit negative deviations from ideal mixing, and for larger ϵ_{AB}, it is clear that the mixtures each possess a minimum-pressure azeotrope. The $\epsilon_{AB} = 1.4$ and 1.6 systems simulated here are nearly azeotropic.

The surface tension as a function of ϵ_{AB} is presented in Figure 10. As A−B attraction is increased from the hard-sphere limit, surface tension decreases as a result of the increased presence of solute in the liquid. Beyond a point, however, further increase in attraction leads to an increase in surface tension. The liquid composition does not vary much across this range because it is almost equal to the overall composition. This increasing surface tension is a result of the greater cohesion of the liquid with the more strongly attractive solute.

Density profiles for a few of these systems are presented in Figure 11. The solute and solvent densities vary identically across the interface, and except for $\epsilon_{AB} = 1.0$, there is no obvious depletion or enhancement of either species at the interface. Thus, the behavior of τ is hard to gauge from these pictures. We present values of τ computed according to the Hansen−Turkevich−Mann formula, eq 8, in Table 2. There is no clear pattern to the behavior, perhaps reflecting that the overall composition is not an especially useful quantity to fix when comparing two systems this way. However, it is notable that the slopes remain negative, except for the two cases that Figure 9 identified as near-azeotropic. The sensitivity analysis shows that τ is very sensitive to some of the properties used in its calculation, such that just a 1% change in the input quantity can lead to more than a 100% variation in τ. However, these input quantities are themselves not subject to much variation, as at the bubble point they are closely connected to the overall composition, which is known exactly. Still, this sensitivity should be kept in mind when considering these results.

To consider further the behavior of τ near an azeotrope, we can perform an asymptotic expansion of eq 8; thus,

$$\tau \sim -\Gamma_2(v^\beta - v^\alpha)\delta^{-1} + O(\delta^0) \qquad (17)$$

where $\delta = 1 - x_1^\beta/x_1^\alpha$. Unfortunately, we cannot gather much insight from this result. It does not give a clear

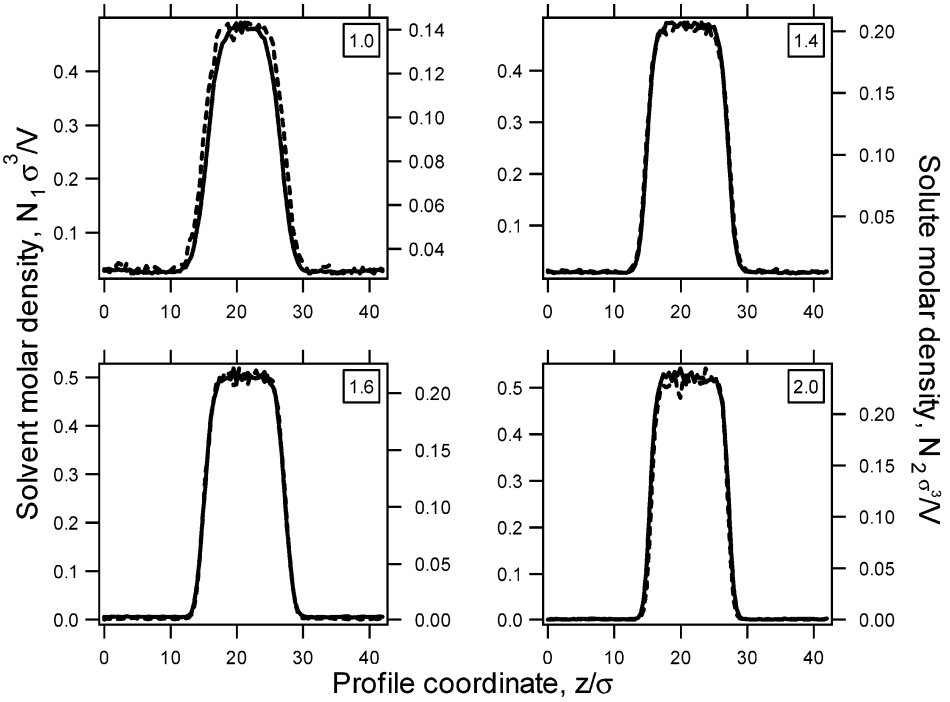

Figure 11. Profiles of solvent molar density (solid line) and solute molar density (dashed line) for various ϵ_{AB} (indicated by the value in the box) at $T = 1.0$. The overall composition (vapor + liquid + interface) for the square-well (A) species is 0.7.

indication of even the expected sign of τ, and while it suggests that τ might diverge at the azeotrope, it may be that Γ_2 vanishes there also, which would negate the basis for the asymptotic form. A similar analysis applied to eq 8 yields

$$\tau \sim -\left(N - \frac{N_1}{x_1^\alpha}\right)(v^\beta - v^\alpha)\delta^{-1} + O(\delta^0) \qquad (18)$$

which also does not lead to a general conclusion. It is hard to gauge the behavior of the first term in parentheses, which captures the surface effects.

IV. Conclusion

The study of simple molecular models can provide qualitative insight regarding the molecular origins of macroscopic behavior. In the present case, we have shown how features of the surface connect to the way vapor−liquid surface tension varies with pressure for two-component mixtures. With the molecular model, we can approach the ideal of an inert gas pressurizing the system. In this case, we observe that the pressure derivative is positive, in agreement with experimental observations that use helium as a pressurizing gas. The addition of modest attraction between the gas and the solvent finds that the pressure derivative takes negative values and that this behavior persists as the solute−solvent attraction is increased. The only exceptional behavior in this regard may be at points of azeotropy, at which we again observe positive derivatives. However, we are not able to conclude that this is a general feature of azeotropic systems.

The present study permits us to examine the relation of the pressure derivative to surface-excess properties. We find that the connection between the derivative and the Gibbs surface excess is in place for the limit in which the solute is insoluble in the solvent. In the more general case, the general surface thermodynamics of Hansen provides an appropriate basis for describing the behavior. We show that the pressure derivative established using this formalism is in good agreement with the observed variation of the surface tension with pressure.

Acknowledgment. This work has been supported by the U.S. National Science Foundation, grants CTS-0076515 and CTS-0219266. Computational resources have been provided by the University at Buffalo Center for Computational Research.

LA0471947